Mass measurements of neutron-rich indium isotopes toward the $N = 82$ shell closure

C. Babcock,[1,*] R. Klawitter,[1,2] E. Leistenschneider,[1,3] D. Lascar,[1,†] B. R. Barquest,[1] A. Finlay,[1,3] M. Foster,[1,4] A. T. Gallant,[1,‡] P. Hunt,[5] B. Kootte,[1,6] Y. Lan,[1,3] S. F. Paul,[1,7] M. L. Phan,[1,3] M. P. Reiter,[1,8] B. Schultz,[1,9] D. Short,[1,10] C. Andreoiu,[10] M. Brodeur,[9] I. Dillmann,[1,11] G. Gwinner,[6] A. A. Kwiatkowski,[1,12] K. G. Leach,[1,5] and J. Dilling[1,3]

[1]*TRIUMF, 4004 Wesbrook Mall, Vancouver, British Columbia V6T 2A3, Canada*
[2]*Max-Planck-Institut für Kernphysik, Heidelberg D-69117, Germany*
[3]*Department of Physics and Astronomy, University of British Columbia, Vancouver, British Columbia V6T 1Z1, Canada*
[4]*Department of Physics, University of Surrey, Guildford GU2 7XH, United Kingdom*
[5]*Department of Physics, Colorado School of Mines, Golden, Colorado 80401, USA*
[6]*Department of Physics and Astronomy, University of Manitoba, Winnipeg, Manitoba R3T 2N2, Canada*
[7]*Ruprecht-Karls-Universität Heidelberg, D-69117 Heidelberg, Germany*
[8]*II. Physikalisches Institut, Justus-Liebig-Universität, 35392 Gießen, Germany*
[9]*Department of Physics, University of Notre Dame, Notre Dame, Indiana 46556, USA*
[10]*Department of Chemistry, Simon Fraser University, Burnaby, British Columbia V5A 1S6, Canada*
[11]*Department of Physics and Astronomy, University of Victoria, Victoria, British Columbia V8P 5C2, Canada*
[12]*Cyclotron Institute, Texas A&M University, College Station, Texas 77843, USA*

(Received 15 December 2017; published 9 February 2018)

Precise mass measurements of the neutron-rich $^{125-130}$In isotopes have been performed with the TITAN Penning trap mass spectrometer. TITAN's electron beam ion trap was used to charge breed the ions to charge state $q = 13+$ thus providing the necessary resolving power to measure not only the ground states but also isomeric states at each mass number. In this paper, the properties of the ground states are investigated through a series of mass differentials, highlighting trends in the indium isotopic chain as compared to its proton-magic neighbor, tin ($Z = 50$). In addition, the energies of the indium isomers are presented. The (8^-) level in ^{128}In is found to be 78 keV lower than previously thought and the $(21/2^-)$ isomer in ^{127}In is shown to be lower than the literature value by more than 150 keV.

DOI: 10.1103/PhysRevC.97.024312

I. INTRODUCTION

Measurements of nuclear masses and the extraction of binding energies provide information on the evolution of nuclear shell structure when studied across isotopic chains. Since binding energies encode all the interactions in a nucleus, careful study of their development as a function of N and Z can give insights into shell structure, single particle energy levels, deformation, and collectivity [1]. Mass measurements also act as important inputs to mass models and nuclear theory. Many mass models (see, for instance, Refs. [2–4]) rely on the accurate determination of binding energies in order to make meaningful predictions of masses further from stability. Such mass values are required for astrophysical calculations, for example of the rapid neutron-capture (r-)process path [5].

In addition to the investigation of ground state properties, precise mass measurements done with Penning traps are currently one of the most powerful methods to search for low-lying, long-lived (ms) isomers populated in the radioactive beam production process [6,7]. Accurate knowledge of isomeric energy levels, particularly near ^{132}Sn, plays an important role in constraining interactions used in shell models and, in certain cases may impact the β-decay path in the r-process [8]. In this region of the nuclear chart, the $\pi 1g_{9/2}$ and $\nu 1h_{11/2}$ orbitals found just below the $Z = 50$ and $N = 82$ shell closures produce isomeric states in many nuclei (for examples, see Refs. [9–11]). The energy levels in many of these states are determined only indirectly (for example through β-decay studies), whereas the more accurate determinations possible with Penning trap mass spectrometry allow information about the evolution of proton and neutron hole states towards ^{132}Sn.

We present here Penning trap mass measurements of indium isotopes in the range $A = 125$–130, along with unambiguous measurements of at least one isomer in each case. For all but ^{129g,m}In [8,12] these are the first direct mass measurements of the ground states and isomers. The indium isotopes are one proton away from the $Z = 50$ (Sn) closed proton shell, and ^{130}In is one neutron away from the $N = 82$ closed neutron shell, making these ideal isotopes to test the development of nuclear shell structure approaching doubly magic ^{132}Sn.

II. EXPERIMENTAL SETUP

This experiment was conducted using TRIUMF's Ion Traps for Atomic and Nuclear science experiment (TITAN) [13],

*Corresponding author: cbabcock@triumf.ca
†Present address: Physics Division, ANL, Argonne, IL 60439, USA.
‡Present address: Lawrence Livermore National Laboratory, Livermore, California 94550, USA.

 ©2018 American Physical Society

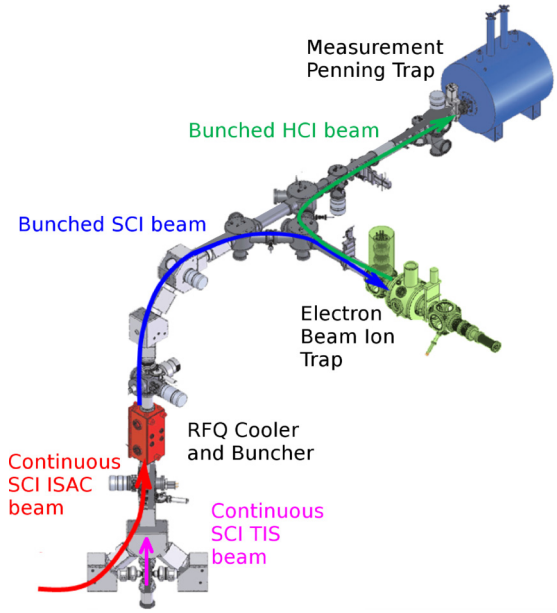

FIG. 1. Layout of the TITAN experiment, showing the three ion traps used for this experiment: the RFQ cooler and buncher, the EBIT charge breeder and the measurement Penning trap. Arrows show the path of the incoming ISAC/TIS beam as well as the singly charged ion (SCI) beam and the highly charged ion (HCI) beam. See text for details.

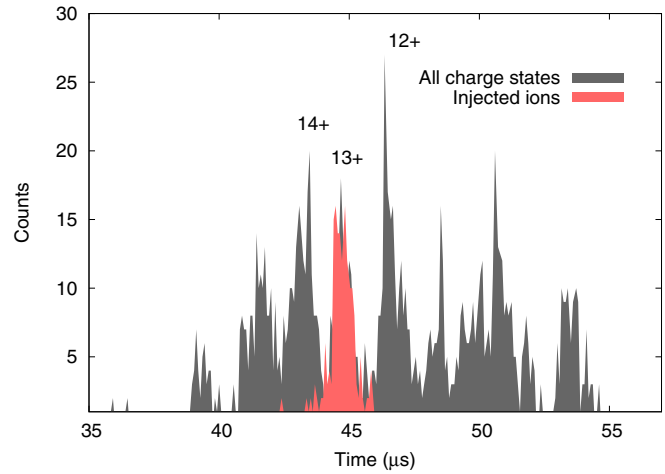

FIG. 2. Time-of-flight spectrum of the beam after extraction from the EBIT (dark gray). The red peak at 13+ indicates the ions selected, using the Bradbury Nielsen gate, for injection into MPET.

located at the Isotope Separator and ACcelerator facility (ISAC) [14]. A 480 MeV beam of protons from the main TRIUMF cyclotron was impinged on a UC_x target, and the resulting indium isotopes were selectively ionized using TRIUMF's Ion Guide Laser Ion Source (IG-LIS). This kind of ion source can suppress surface ionized isobaric contaminants by up to seven orders of magnitude [15]. The beam was then mass separated using the ISAC magnetic separator (resolving power $R = 2000$ [16]) and delivered to the TITAN experiment in the ISAC experimental hall. At the bottom of the beamline there is a hot-filament ion source [17] (TITAN Ion Source, TIS) which is used to provide stable calibrant ions for mass measurements. The layout of the experiment is shown in Fig. 1.

The continuous beam from ISAC or TIS was cooled and bunched in TITAN's radio frequency quadrupole cooler and buncher (RFQ) [18], a helium-filled Paul trap, before being sent to the electron beam ion trap (EBIT) [19]. In this experiment, the EBIT was used to increase the charge state of the indium ions, and a charge state of 13+ was selected and sent to the measurement Penning trap (MPET) [20] for mass measurement. TITAN's EBIT consists of a hot cathode electron gun which produces electrons via thermionic emission, a superconducting magnet which serves to compress the electron beam as it leaves the cathode, and a collector segment which acts as an electron beam dump to prevent the electrons from leaving the EBIT. The ion bunch from the RFQ cooler/buncher entered the EBIT and was trapped axially in an electrostatic potential well located at the center of the magnet. Radial trapping was accomplished by the space charge potential of the electron beam and, to a lesser extent by the magnetic field. In the trapping region, the ion bunch was overlapped with the electron beam and the charge state of the ions was increased over time via electron impact ionization [21].

To achieve the desired charge state, the EBIT magnet was operated at 4.5 T with an electron beam current of 100 mA and an electron beam energy around 4 keV. A significant ion population reached the desired charge state, $q = 13+$, in about 10 ms, after which the bunch was ejected from the EBIT. The different charge states produced in the charge breeding process were separated from one another based on time-of-flight using a Bradbury Nielsen gate [22]. The 13+ charge state was selected in order to take advantage of a region of low background in the EBIT time-of-flight spectrum, an example of which is shown in Fig. 2. The single A/q bunch was then injected into MPET for RF excitation.

Once the ions were trapped in MPET, we used the time-of-flight ion-cyclotron-resonance (ToF-ICR) [23] technique to determine their cyclotron frequency. A radio frequency pulse was applied to the trap electrodes for 50–200 ms in order to resonantly excite the motion of the ion. The ion's time-of-flight from the trap to a detector was then measured. Sweeping the frequency produced a minimum in the time-of-flight at the cyclotron frequency of the ion, and this frequency was determined by fitting the theoretical curve shape [24] to the data from the frequency sweep. An example of the data obtained in a frequency sweep for ^{128g,m}In is shown in Fig. 3. The figure shows a double resonance and the theoretical fit to the data.

The mass is extracted from the cyclotron frequency using the relationship

$$\nu_c = \frac{qeB}{2\pi m}, \tag{1}$$

where q is the charge state of the ion, e is the elementary charge, B is the magnetic field in the trap center, and m is the ion mass.

TITAN's unique setup, which couples an EBIT to a Penning trap, means that highly charged ions can be used to increase the precision of a mass measurement. The statistical uncertainty

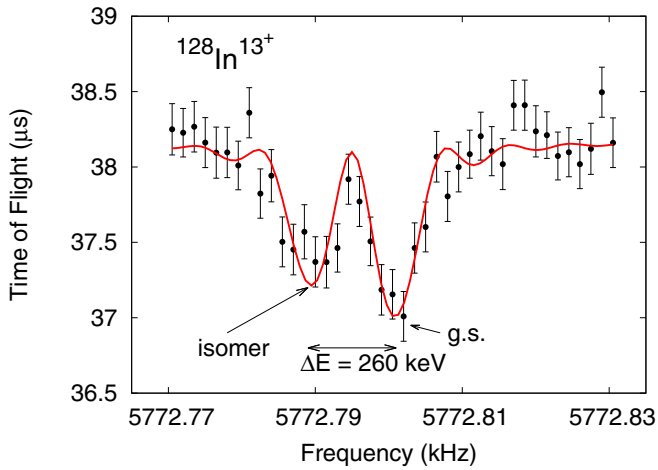

FIG. 3. Time of flight resonance for ^{128}In^{13+}, showing the ground state and isomer. The excitation time was 125 ms. The line shows the fit to the data.

on a Penning trap mass measurement is given by [25]

$$\frac{\delta m}{m} = \frac{\gamma\, m}{qeBt_{\rm rf}\sqrt{N_{\rm ion}}}, \tag{2}$$

where γ is a setup-dependent quality factor typically on the order of 1 (see [26]), $t_{\rm rf}$ is the excitation time in the Penning trap and $N_{\rm ion}$ is the number of ions observed. At a radioactive beam facility, where the number of ions is limited by the production rate and the excitation time is limited by the half-life of the exotic isotopes, an increase in q is the most effective way to gain precision and resolving power.

III. RESULTS

Equation (1) shows that in order to determine the mass, the magnetic field sampled by the ions must be known. To determine this to the required accuracy and to account for any changes in the magnetic field over the course of the experiment, the cyclotron frequency of a calibrant ion with a well-known mass, sampling the same field as the ion of interest, was measured before and after the measurement of each indium isotope. The mass of the ion of interest was then calculated as a ratio with the calibrant

$$R = \frac{\nu_{c,\rm cal}}{\nu_c} = \frac{q_{\rm cal}m}{qm_{\rm cal}}. \tag{3}$$

In this experiment, ^{133}Cs^{13+} produced by TITAN's offline ion source was used as a calibrant ion. The mass of the neutral indium atom is then given by

$$m = \frac{q}{q_{\rm cal}}R(m_{\rm cal} - q_{\rm cal}m_e + B_{e,\rm cal}) + qm_e - B_e, \tag{4}$$

where m_e is the electron mass and B_e is the electron binding energy for the chosen charge state [27].

Systematic effects that may shift the measured mass have been well studied at TITAN [28]. Sources of error relating to the construction and setup of the trap, such as inhomogeneities in the magnetic field, distortions in the harmonic potential and a possible misalignment of the electric and magnetic fields, have been studied based on the work in [29] and found to be in the range of $\Delta R/R \sim 10^{-9}$. Sources of error independent of the setup construction, such as non-linear fluctuations in the magnetic field, relativistic effects, and ion-ion interactions, have also been considered. Nonlinear fluctuations and relativistic effects have been calculated to be on the order of $\Delta R/R \sim 5 \times 10^{-10}$ and $\Delta R/R \sim 9 \times 10^{-10}$, respectively. Errors resulting from the interactions of multiple ions in the trap are minimized by keeping the count rate low, however, this effect was investigated using a count class analysis [30]. Where sufficient statistics were available, this analysis gave a ratio shift of $\Delta R/R \sim 10^{-10}$. In this experiment, precisions on the order of $\Delta R/R \sim 10^{-7}$ were required and thus these systematic errors are negligible.

Table I shows the ratios [Eq. (3)], mass excesses and excitation energies of the isotopes and isomers measured in this experiment. The TITAN mass excesses and those from the AME2016 [31] agree to within 2σ in all cases except for

TABLE I. Shown here are the half-lives [32], spin/parity assignments [32], ratios, mass excesses (M.E.), and excitation energies for the measured isotopes $^{125-130}$In and their isomers. For comparison, the mass excesses taken from the AME2016 [31] for the ground states and from NUBASE2016 [33] for the isomeric states are also listed, along with the ENSDF energy levels.

Isotope	$t_{1/2}$ [s]	J^π	Ratio ($\nu_{c,\rm cal}/\nu_c$)	TITAN [keV/c^2]	AME2016 [keV/c^2]	Exc. E [keV]	Lit. [keV]
^{125}In	2.36(4)	$9/2^+$	0.939865469(14)	−80412.4(15)	−80477(27)	0.0	0.0
^{125m}In	12.2(2)	$1/2^{(-)}$	0.93986831(10)	−80061(13)	−80117(27)	351(13)	360.12(9)
^{126}In	1.53(1)	$3^{(+)}$	0.947411045(34)	−77809.5(41)	−77773(27)	0.0	0.0
^{126m}In	1.64(5)	(8^-)	0.947411771(41)	−77719.6(50)	−77710(50)	89.9(65)	102(64)
^{127}In	1.09(1)	$9/2^+$	0.954943129(87)	−76876(11)	−76896(21)	0.0	0.0
^{127m1}In	3.67(4)	$(1/2^-)$	0.95494628(12)	−76487(15)	−76487(21)	390(18)	408.9(3)
^{127m2}In	1.04(10)	$(21/2^-)$	0.95495684(39)	−75179(48)	−75030(60)	1697(49)	1863(58)
^{128}In	0.84(6)	$(3)^+$	0.962489530(79)	−74170.5(97)	−74146(153)	0.0	0.0
^{128m}In	0.72(10)	(8^-)	0.962491653(74)	−73908.8(91)	−74060(30)	262(13)	340(60)
^{129}In	0.611(5)	$9/2^+$	0.970024865(50)	−72836.4(61)	−72838(3)	0.0	0.0
^{129m}In	1.23(3)	$(1/2^-)$	0.97002845(11)	−72392(14)	−72380(3)	444(15)	451(1)
^{130}In	0.29(2)	$1^{(-)}$	0.97757344(16)	−69862(20)	−69883(38)	0.0	0.0
^{130m}In	0.54(1)	(5^+)	0.97757633(23)	−69503(28)	−69480(50)	359(34)	400(60)

^{128m}In, and the agreement for the only isotope with a previous Penning trap measurement, ^{129}In, is very good. TITAN has decreased the errors on the other ground state mass excesses, particularly for ^{125}In and ^{128}In, where the AME2016 error is reduced from 27 keV/c^2 to 1.5 keV/c^2 and from 153 keV/c^2 to 9.7 keV/c^2, respectively. For the measurements of the isomers, the TITAN errors also improve the NUBASE2016 [33] values, most notably for ^{126m}In where the error is reduced by an order of magnitude.

In total, six different isotopes were measured, each with at least one isomer and, in the case of ^{127}In, two isomers. Except for ^{129}In, these are the first direct mass measurements of the ground and isomeric states of these isotopes, which accounts for the significant reduction of uncertainties. The use of the EBIT to raise the charge states of the ions not only reduces the uncertainty on the mass measurement, but provides the resolution necessary to separate these low-lying isomers, which are otherwise inaccessible to conventional mass measurement techniques. However, it must be noted that ^{130}In has a low-lying (10^-) isomer at 50(50) keV [33] which could not be resolved in this experiment. This isomer has a half-life of 540(1) ms (a combined value for this isomer and the (5^+) isomer at 400 keV), and thus, if it was produced in the target, our ground state measurement could be a convolution of the ground state and this isomer.

IV. DISCUSSION

Ground state properties are commonly investigated through binding energy difference formulas, such as the two-neutron separation energy

$$S_{2n} = \text{B.E.}(Z,N) - \text{B.E.}(Z,N-2), \tag{5}$$

where B.E. is the binding energy. This can be used to highlight changes in shell structure and single particle energy levels across an isotopic chain. Figure 4 shows the S_{2n} values for several isotopic chains near indium. The general trend in two-neutron separation energies shows a decrease as the neutron shell is filled and a sharp inflection point at a magic number. Deviations from a linear decrease indicate possible changes to the shell structure.

In Fig. 4, the In values can be seen to decrease relatively steadily towards the $N = 82$ shell gap, except for a slight elevation at $N = 77$ and $N = 79$. Hints of this pattern can be seen in the Cd nuclei as well, however large uncertainties on the masses below Cd ($Z = 48$) make comparisons with lower proton numbers difficult. In contrast, the proton-magic Sn isotopes, spherical near doubly magic ^{132}Sn, show the expected linear decrease. The deviations observed in the In S_{2n} curve may hint at changes in the single particle levels expected for these nuclei.

We can further investigate the shell structure in these isotopes using higher-order binding energy differentials to isolate the role played by specific contributions to the total interaction energy. One such differential is the empirical neutron pairing gap, given by [34]

$$\Delta_n^3(Z,N) = \frac{(-1)^N}{2}(2\text{B.E.}(Z,N) - \text{B.E.}(Z,N+1) - \text{B.E.}(Z,N-1)). \tag{6}$$

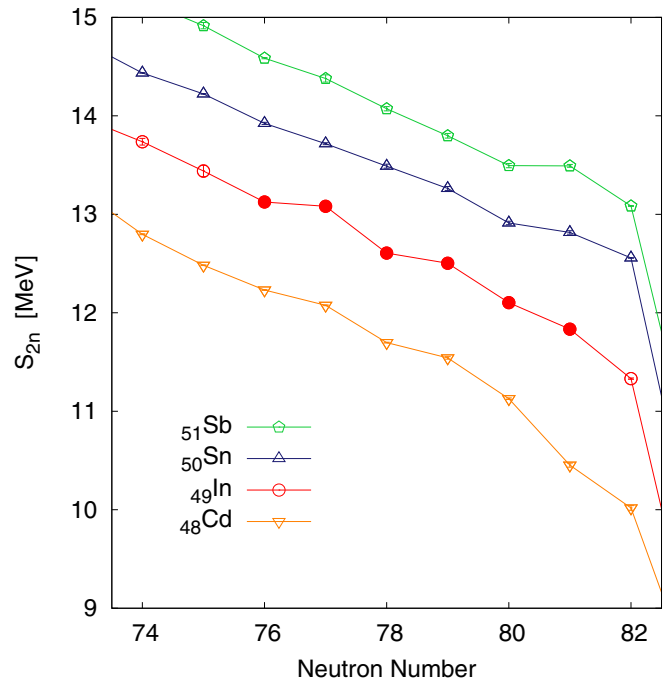

FIG. 4. Two-neutron separation energies for the isotopic chains of Cd, In, Sn, and Sb. The filled circles show the values derived from this experiment, while other values are taken from the AME2016 [31].

This encodes the odd-even staggering between nuclei of different A and thus an approximation of the contribution of proton-proton or neutron-neutron pairing to the binding energy can be made. Figure 5 shows the results for the Sn isotopes (even Z) and the In isotopes (odd Z). The values for indium follow those of tin up to around $N = 77$, after which they begin to decrease faster, producing larger gaps between the two curves as we move towards $N = 82$. This may indicate a difference in the filling of the protons, which should, in

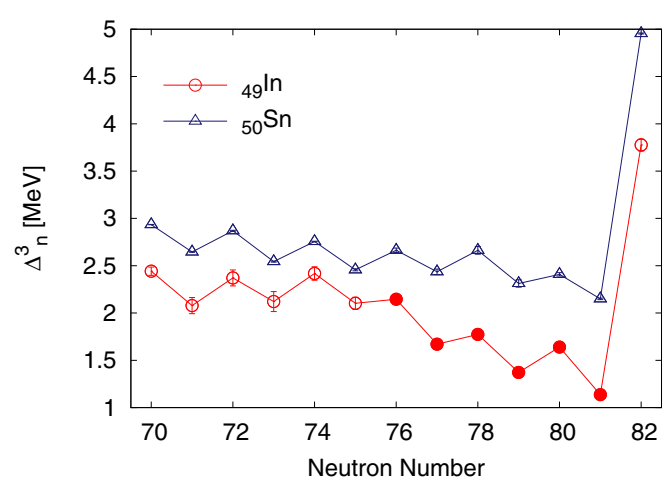

FIG. 5. The empirical pairing gap, Δ_n^3, for indium and tin isotopes in the mass region of interest. Filled circles show the pairing gaps derived from our measurements, while other values are taken from the AME2016 [31].

principle, be in the $\pi g_{9/2}$ level. However, the general trend of the indium isotopes towards $N = 82$ follows that of the tin isotopes.

We can examine the influence of proton-neutron correlations in these nuclei using another higher-order differential, δV_{pn} [35], given by

$$\delta V_{pn}^{oe} = \tfrac{1}{2}(\text{B.E.}(Z,N) - \text{B.E.}(Z,N-2)) - (\text{B.E.}(Z-1,N) - \text{B.E.}(Z-1,N-2)), \quad (7)$$

$$\delta V_{pn}^{oo} = (\text{B.E.}(Z,N) - \text{B.E.}(Z,N-1)) - (\text{B.E.}(Z-1,N) - \text{B.E.}(Z-1,N-1)), \quad (8)$$

where *oe* indicates nuclei with odd Z, even N and *oo* indicates nuclei with both Z and N odd. Associated with the interactions of the last protons and neutrons in a nucleus, it has been shown to be entirely related to the isoscalar $T = 0$ component of the residual interaction [36]. The $T = 0$ part of the *pn* interaction plays a vital role in configuration mixing, deformation and collectivity [35] and thus it contains indirect information on the structure of the single particle levels [37]. It is also useful as an input to mass models which do not take proton-neutron interactions explicitly into account.

Since the binding energy encodes the sum of all interactions within a nucleus, the efficacy of this method relies on certain simplifications. If the nuclear wave function is dominated by one orbital, as is often the case near shell closures, δV_{pn} effectively probes the average correlations between the valence protons and neutrons. However, if there is extensive mixing in the wave function, often found towards midshell, more complex calculations are required [38]. In the case of the indium isotopes, the nuclei under investigation are one proton away from the $Z = 50$ shell closure (filling the $\pi g_{9/2}$ orbital), and one to six neutrons away from the $N = 82$ shell closure (filling the $\nu h_{11/2}$, $\nu d_{3/2}$, or $\nu s_{1/2}$ orbitals). As there are no signs of intruder orbitals up to ^{127}In [39] and our S_{2n} results show no dramatic deviations from the Sn isotopes, this metric should allow us to draw general conclusions about the interactions of valence protons and neutrons. Figure 6 shows δV_{pn} calculated for In and Sn.

The features of this plot can be qualitatively explained by considering the known properties of the *pn* interaction. The possible subshell effects which have been discussed in relation to S_{2n} and Δ_n^3 are brought about in large part by the short-range, monopole component of the *pn* interaction. This part of the *pn* interaction has a dependence on the orbital occupation of the nucleons [40]. Interactions between valence protons and neutrons are strongest when the neutron and proton wave functions have the largest spatial overlap. For the indium isotopes, the protons occupy the $\pi g_{9/2}$ shell immediately below $Z = 50$ while the neutrons occupy the $\nu h_{11/2}$, $\nu d_{3/2}$, and $\nu s_{1/2}$ shells below $N = 82$. Though the protons and neutrons occupy different major shells, the high symmetry between the *pf* shell and the *gd* shell means that the proton and neutron wave functions have a high overlap, producing a strong *pn* interaction. For the indium chain, this culminates in the one-hole one-hole ($\pi g_{9/2} \otimes \nu h_{11/2}$) configuration of ^{130}In, where we see the maximum δV_{pn} in Fig. 6. Indeed, this is a large

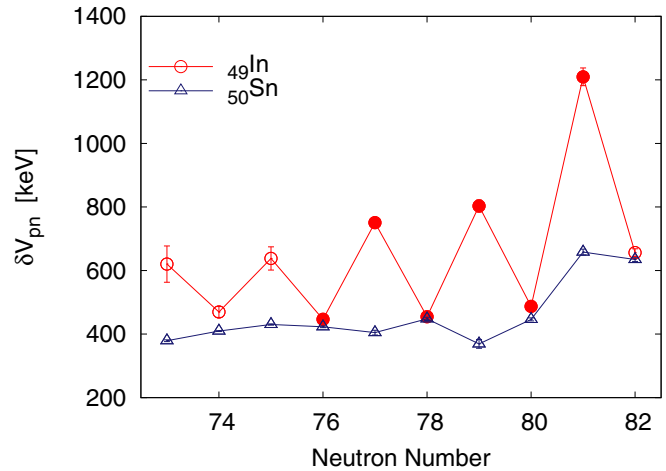

FIG. 6. δV_{pn} for indium and tin isotopes in the mass region of interest. Filled circles show the values derived from our measurements, while other values are taken from the AME2016 [31].

value compared to other odd-Z isotopes near shell closures. $^{206}_{81}$Tl$_{125}$, which, like $^{130}_{49}$In$_{81}$ is one proton and one neutron away from a doubly-magic nucleus, has a δV_{pn} of 835 keV based on data from the AME2016. Interpretation of this high value will require more detailed studies.

The lower δV_{pn} values at $N = 75,77,79$ reflect less overlap between the wave functions and may indicate a shift in the proton or neutron levels further away from the $N = 82$ closure. From the ground state spins, we can infer that the $\nu h_{11/2}$ and $\nu d_{3/2}$ levels in tin cross at ^{127}Sn ($N = 77$). In indium, this may occur at ^{128}In ($N = 79$), where the ground state spin changes from 3^+, built on a $[\pi(g_{9/2})^{-1}\nu(d_{3/2})]$, state to 1^-, built on a $[\pi(g_{9/2})^{-1}\nu(h_{11/2})^{-1}]$ state in ^{130}In. There are also ambiguities in the Cd chain spins for this mass region, with theory predicting alternately an 11/2 and a 3/2 ground state in the odd-A isotopes (see, for instance, [41,42]). δV_{pn} values for the Cd chain isotopes are not shown, since they depend on the binding energies of neutron-rich Pd ($Z = 46$) isotopes which have not been measured. The magnitude of the odd-even staggering observed in odd-Z nuclei is still a topic of interest, however it appears to be related to increased binding energy in both odd-odd and even-even nuclei [43,44].

While the binding energies presented here have been used to illuminate important properties of the ground states of these isotopes, the added resolving power achieved with highly charged ions allows TITAN to probe the properties of low-lying isomers as well. In this study, isomers were observed and resolved in each of the isotopes $^{125-130}$In. Figure 7 shows their energy levels. It can be seen from the spins and parities that the high ΔJ values between the measured levels make these excitation energies challenging to determine with decay spectroscopy due to the forbidden nature of the transitions. Thus the detection of isomers using highly charged ions at TITAN provides a complementary method to other detection techniques.

The comparison to the ENSDF values shows good agreement, with the exception of the (8^-) isomer in ^{128}In [45] and the ($21/2^-$) isomer in ^{127}In [9], both previously determined

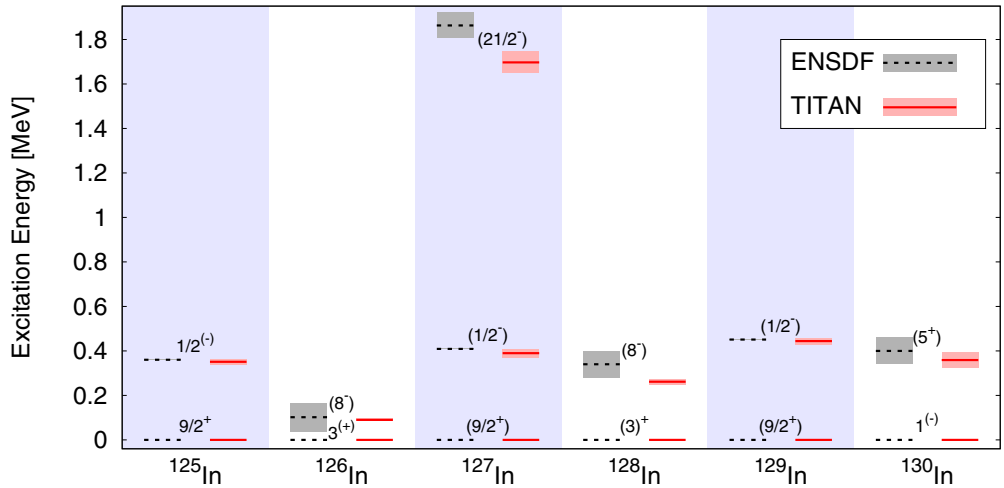

FIG. 7. Energy levels of ground states and isomers measured in this experiment (solid red line) compared to the literature values (dashed black line) taken from ENSDF [32]. The size of the shaded bar represents the error on the value. The spin and parity assignments are also taken from ENSDF.

through $\beta\gamma$-coincidence measurements. The TITAN measurement puts the (8^-) level 78 keV lower than the ENSDF value, while the $(21/2^-)$ level is revised downwards by more than 150 keV.

V. CONCLUSIONS

This paper reports new measurements of the masses of $^{125-130}$In and their isomers with the TITAN Penning trap mass spectrometer. For five of the isotopes these are the first direct measurements. In addition, the use of the TITAN EBIT charge breeder to increase the charge state of the indium ions has resulted in the resolving power necessary to unambiguously identify the energy level of at least one isomer at each mass number. The ground state properties of these isotopes have been investigated using the two-neutron separation energy, the empirical pairing gap, and the empirical *pn* interaction. Trends in these binding energy differentials have shown no signs of deviation from sphericity for these nuclei, though there is a re-ordering of single particle energies as neutrons are removed from the $N = 82$ closed shell. The high values calculated for δV_{pn} suggest that the *pn* interaction may play a large role for these isotopes. In addition, the measured energies of several isomers were compared to literature values, and those of ^{127m2,128m}In were found to be lower than previously thought, suggesting modifications to the decay chains for these isotopes.

Future work at TITAN will benefit from two methods of producing cleaner, more intense exotic beams. The first is the installation of a multiple reflection time-of-flight mass spectrometer [46], which will improve the purity of the beam sent to MPET, as well as making mass measurements of species with very low production rates possible. The second is the completion of the advanced rare isotope lab (ARIEL) at TRIUMF, which will bring significant advances in the production and separation of increasingly exotic beams [47].

ACKNOWLEDGMENTS

TRIUMF receives federal funding via a contribution agreement with the National Research Council of Canada (NRC). This work was partially supported by the Natural Sciences and Engineering Research Council of Canada (NSERC), the Canada Foundation for Innovation (CFI), the US National Science Foundation under Grant No. PHY-1419765, the U.S. Department of Energy under Grant No. DE-SC0017649, the Deutsche Forschungsgemeinschaft (DFG, Germany) under Grant No. FR 601/3-1, Brazil's Conselho Nacional de Desenvolvimento Científico e Technológico (CNPq), and the BMBF (Germany) under Contract No. 05P15RGFN1.

[1] D. Lunney, J. M. Pearson, and C. Thibault, Rev. Mod. Phys. **75**, 1021 (2003).
[2] P. Möller, A. Sierk, T. Ichikawa, and H. Sagawa, At. Data Nucl. Data Tables **109–110**, 1 (2016).
[3] S. Goriely, N. Chamel, and J. M. Pearson, Phys. Rev. C **88**, 024308 (2013).
[4] J. Duflo and A. P. Zuker, Phys. Rev. C **52**, R23 (1995).
[5] F.-K. Thielemann, A. Arcones, R. Käppeli, M. Liebendörfer, T. Rauscher, C. Winteler, C. Fröhlich, I. Dillmann, T. Fischer, G. Martinez-Pinedo, K. Langanke, K. Farouqi, K.-L. Kratz, I. Panov, and I. Korneev, Prog. Part. Nucl. Phys. **66**, 346 (2011).
[6] A. T. Gallant, M. Brodeur, T. Brunner, U. Chowdhury, S. Ettenauer, V. V. Simon, E. Mané, M. C. Simon, C. Andreoiu, P. Delheij, G. Gwinner, M. R. Pearson, R. Ringle, and J. Dilling, Phys. Rev. C **85**, 044311 (2012).
[7] M. Block, C. Bachelet, G. Bollen, M. Facina, C. M. Folden, C. Guénaut, A. A. Kwiatkowski, D. J. Morrissey, G. K. Pang, A. Prinke, R. Ringle, J. Savory, P. Schury, and S. Schwarz, Phys. Rev. Lett. **100**, 132501 (2008).

[8] A. Kankainen, J. Hakala, T. Eronen, D. Gorelov, A. Jokinen, V. S. Kolhinen, I. D. Moore, H. Penttilä, S. Rinta-Antila, J. Rissanen, A. Saastamoinen, V. Sonnenschein, and J. Äystö, Phys. Rev. C **87**, 024307 (2013).

[9] H. Gausemel, B. Fogelberg, T. Engeland, M. Hjorth-Jensen, P. Hoff, H. Mach, K. A. Mezilev, and J. P. Omtvedt, Phys. Rev. C **69**, 054307 (2004).

[10] L. Spanier, K. Aleklett, B. Ekström, and B. Fogelberg, Nucl. Phys. A **474**, 359 (1987).

[11] D. S. Judson, A. M. Bruce, T. Kibédi, G. D. Dracoulis, A. P. Byrne, G. J. Lane, K. H. Maier, C.-B. Moon, P. Nieminen, J. N. Orce, and M. J. Taylor, Phys. Rev. C **76**, 054306 (2007).

[12] J. Hakala, J. Dobaczewski, D. Gorelov, T. Eronen, A. Jokinen, A. Kankainen, V. S. Kolhinen, M. Kortelainen, I. D. Moore, H. Penttilä, S. Rinta-Antila, J. Rissanen, A. Saastamoinen, V. Sonnenschein, and J. Äystö, Phys. Rev. Lett. **109**, 032501 (2012).

[13] A. Kwiatkowski, T. Macdonald, C. Andreoiu, J. Bale, T. Brunner, A. Chaudhuri, U. Chowdhury, S. Ettenauer, A. Gallant, A. Grossheim, A. Lennarz, E. Mané, M. Pearson, B. Schultz, M. Simon, V. Simon, and J. Dilling, Nucl. Instrum. Methods Phys. Res. B **317**, 517 (2013); XVIth International Conference on ElectroMagnetic Isotope Separators and Techniques Related to their Applications, December 2–7, 2012 at Matsue, Japan.

[14] M. Dombsky, D. Bishop, P. Bricault, D. Dale, A. Hurst, K. Jayamanna, R. Keitel, M. Olivo, P. Schmor, and G. Stanford, Rev. Sci. Instrum. **71**, 978 (2000).

[15] S. Raeder, H. Heggen, J. Lassen, F. Ames, D. Bishop, P. Bricault, P. Kunz, A. Mjøs, and A. Teigelhöfer, Rev. Sci. Instrum. **85**, 033309 (2014).

[16] P. G. Bricault, F. Ames, M. Dombsky, P. Kunz, and J. Lassen, Hyperfine Interact. **225**, 25 (2014).

[17] A. A. Kwiatkowski, C. Andreoiu, J. C. Bale, T. Brunner, A. Chaudhuri, U. Chowdhury, P. Delheij, S. Ettenauer, D. Frekers, A. T. Gallant, A. Grossheim, G. Gwinner, F. Jang, A. Lennarz, T. Ma, E. Mané, M. R. Pearson, B. E. Schultz, M. C. Simon, V. V. Simon, and J. Dilling, Hyperfine Interact. **225**, 143 (2014).

[18] T. Brunner, M. Smith, M. Brodeur, S. Ettenauer, A. Gallant, V. Simon, A. Chaudhuri, A. Lapierre, E. Mané, R. Ringle, M. Simon, J. Vaz, P. Delheij, M. Good, M. Pearson, and J. Dilling, Nucl. Instrum. Methods Phys. Res. A **676**, 32 (2012).

[19] A. Lapierre, M. Brodeur, T. Brunner, S. Ettenauer, A. Gallant, V. Simon, M. Good, M. Froese, J. C. López-Urrutia, P. Delheij, S. Epp, R. Ringle, S. Schwarz, J. Ullrich, and J. Dilling, Nucl. Instrum. Methods Phys. Res. A **624**, 54 (2010).

[20] J. Dilling, P. Bricault, M. Smith, and H.-J. Kluge, Nucl. Instrum. Methods Phys. Res. B **204**, 492 (2003); 14th International Conference on Electromagnetic Isotope Separators and Techniques Related to their Applications.

[21] F. Currell and G. Fussmann, IEEE Trans. Plasma Sci. **33**, 1763 (2005).

[22] T. Brunner, A. Mueller, K. O'Sullivan, M. Simon, M. Kossick, S. Ettenauer, A. Gallant, E. Mané, D. Bishop, M. Good, G. Gratta, and J. Dilling, Int. J. Mass Spectrom. **309**, 97 (2012).

[23] G. Bollen, R. B. Moore, G. Savard, and H. Stolzenberg, J. Appl. Phys. **68**, 4355 (1990).

[24] M. Kretzschmar, Phys. Scr. **46**, 555 (1992).

[25] G. Bollen, Nucl. Phys. A **693**, 3 (2001), Radioactive Nuclear Beams.

[26] R. Ringle, G. Bollen, A. Prinke, J. Savory, P. Schury, S. Schwarz, and T. Sun, Nucl. Instrum. Methods Phys. Res. A **604**, 536 (2009).

[27] 2014 CODATA Recommended Values (Online), available http://physics.nist.gov/cuu/Constants (2017, Oct. 18), Physical Measurement Laboratory of the National Institute of Standards and Technology, Gaithersburg, MD (2014).

[28] M. Brodeur, First direct mass measurement of the two and four neutron halos ^{6}He and ^{8}He using the TITAN Penning trap mass spectrometer, Ph.D. thesis, University of British Columbia (2010).

[29] M. Brodeur, T. Brunner, C. Champagne, S. Ettenauer, M. Smith, A. Lapierre, R. Ringle, V. L. Ryjkov, G. Audi, P. Delheij, D. Lunney, and J. Dilling, Phys. Rev. C **80**, 044318 (2009).

[30] A. Kellerbauer, K. Blaum, G. Bollen, F. Herfurth, H.-J. Kluge, M. Kuckein, E. Sauvan, C. Scheidenberger, and L. Schweikhard, Eur. Phys. J. D **22**, 53 (2003).

[31] M. Wang, G. Audi, F. Kondev, W. Huang, S. Naimi, and X. Xu, Chin. Phys. C **41**, 030003 (2017).

[32] M. Bhat, evaluated nuclear structure data file (ENSDF) (1992), data extracted using the NNDC On-Line Data Service from the ENSDF database, file revised as of Oct. 15, 2017.

[33] G. Audi, F. Kondev, M. Wang, W. Huang, and S. Naimi, Chin. Phys. C **41**, 030001 (2017).

[34] W. Satuła, J. Dobaczewski, and W. Nazarewicz, Phys. Rev. Lett. **81**, 3599 (1998).

[35] J.-Y. Zhang, R. Casten, and D. Brenner, Phys. Lett. B **227**, 1 (1989).

[36] D. Brenner, C. Wesselborg, R. Casten, D. Warner, and J.-Y. Zhang, Phys. Lett. B **243**, 1 (1990).

[37] W.-T. Chou, J.-Y. Zhang, R. Casten, and D. Brenner, Phys. Lett. B **255**, 487 (1991).

[38] M. Bender and P.-H. Heenen, Phys. Rev. C **83**, 064319 (2011).

[39] J. Eberz, U. Dinger, G. Huber, H. Lochmann, R. Menges, R. Neugart, R. Kirchner, O. Klepper, T. Kühl, D. Marx, G. Ulm, and K. Wendt, Nucl. Phys. A **464**, 9 (1987).

[40] R. F. Casten, J. Phys. G **14**, S71 (1988).

[41] D. T. Yordanov, D. L. Balabanski, J. Bieroń, M. L. Bissell, K. Blaum, I. Budinčević, S. Fritzsche, N. Frömmgen, G. Georgiev, C. Geppert, M. Hammen, M. Kowalska, K. Kreim, A. Krieger, R. Neugart, W. Nörtershäuser, J. Papuga, and S. Schmidt, Phys. Rev. Lett. **110**, 192501 (2013).

[42] D. Lascar, R. Klawitter, C. Babcock, E. Leistenschneider, S. R. Stroberg, B. R. Barquest, A. Finlay, M. Foster, A. T. Gallant, P. Hunt, J. Kelly, B. Kootte, Y. Lan, S. F. Paul, M. L. Phan, M. P. Reiter, B. Schultz, D. Short, J. Simonis, C. Andreoiu, M. Brodeur, I. Dillmann, G. Gwinner, J. D. Holt, A. A. Kwiatkowski, K. G. Leach, and J. Dilling, Phys. Rev. C **96**, 044323 (2017).

[43] G. J. Fu, J. J. Shen, Y. M. Zhao, and A. Arima, Phys. Rev. C **87**, 044309 (2013).

[44] G. J. Fu, Y. Y. Cheng, H. Jiang, Y. M. Zhao, and A. Arima, Phys. Rev. C **94**, 024312 (2016).

[45] U. Stöhlker, A. Blönnigen, W. Lippert, and H. Wollnik, Z. Phys. A **336**, 369 (1990).

[46] C. Jesch, T. Dickel, W. R. Plaß, D. Short, S. Ayet San Andres, J. Dilling, H. Geissel, F. Greiner, J. Lang, K. G. Leach, W. Lippert, C. Scheidenberger, and M. I. Yavor, Hyperfine Interact. **235**, 97 (2015).

[47] *ISAC and ARIEL: The TRIUMF Radioactive Beam Facilities and the Scientific Program*, edited by J. Dilling, R. Krücken, and L. Merminga (Springer, Berlin, 2014).